Materials Chemistry and Physics 225 (2019) 292–297

Contents lists available at ScienceDirect

Materials Chemistry and Physics

journal homepage: www.elsevier.com/locate/matchemphys

Dimethylsulfoxide as a media for one-stage synthesis of the Fe_3O_4-Based ferrofluids with a controllable size distribution

V.L. Kirillov[a], S.S. Yakushkin[a,*], D.A. Balaev[b], A.A. Dubrovskiy[b], S.V. Semenov[b], Yu.V. Knyazev[b], O.A. Bayukov[b], D.A. Velikanov[b], D.A. Yatsenko[a], O.N. Martyanov[a]

[a] Boreskov Institute of Catalysis, Russian Academy of Sciences, Siberian Branch, Novosibirsk, 630090, Russia
[b] Kirensky Institute of Physics, Federal Research Center KSC SB RAS, Krasnoyarsk, 660036, Russia

HIGHLIGHTS

- One-step synthesis of concentrated magnetite/dimethylsulfoxide ferrofluid.
- Room-temperature hysteresis caused by the interparticle magnetic interactions.
- Initial stages of the colloid formation and the agglomeration process study.

ARTICLE INFO

Keywords:
Ferrofluid
Magnetite nanoparticles
One-step synthesis
Superparamagnetic nanoparticles
Ferromagnetic resonance

ABSTRACT

The ultrafine (d = 4 nm) magnetite ferrofluid with a narrow nanoparticle size distribution has been synthesized in one stage at room temperature from a solution of iron(II) and (III) chlorides in dimethylsulfoxide (DMSO) with the propylene epoxide admixture. This is the first example of obtaining a stable concentrated ultrafine magnetite/DMSO ferrofluid at room temperature. X-ray diffraction, transmission electron microscopy, ferromagnetic resonance, Mössbauer spectroscopy, and magnetostatic study have been used to elucidate the role of DMSO and the H_2O/DMSO ratio in the formation of a stable colloid with a desired nanoparticle size. The initial stages of the magnetite nanoparticles formation have been investigated by the ferromagnetic resonance technique.

1. Introduction

In the last few decades, a great variety of techniques, including hydrothermal/solvothermal synthesis [1–5], microwave synthesis [6], ball milling grinding, and ultrasonication [7–9], have been developed to obtain ferrofluids with a required particle size and desired properties. These techniques are generally divided into one- and two-stage [10]. One of the simplest ways of preparing magnetic nanoparticles is chemical co-precipitation [11] widely used to synthesize magnetite and mixed oxide nanoparticles. The method consists in co-precipitation of the Fe^{2+} and Fe^{3+} salts in an aqueous solution under alkaline conditions [12–15]. Unfortunately, this method does not allow the nanoparticle size distribution to be appropriately controlled.

To prevent agglomeration of nanoparticles and their uncontrolled growth during the synthesis [9], special additives and surfactants [16] are used, which stabilize a colloid system at the second stage of the ferrofluid synthesis. In addition, there are many methods for preparing colloids with the low magnetic nanoparticle content that include an additional centrifugation stage, which ensures a narrow nanoparticle size distribution [11].

Earlier we proposed an elegant method for controlling the magnetic nanoparticle size during the synthesis [17]. In that method, co-precipitation proceeds in the presence of citrate ions, which act as a surfactant, covering the synthesized nanoparticles to limit their growth. The proposed method allows one to produce nanoparticles of desired size by controlling the citrate ions concentration, in a diluted water solution (< 0.2 vol%), however at higher concentration the aggregation of nanoparticles takes place [17]. The main reason of agglomeration in this case is the Cl−anions; if their concentration is higher than critical coagulation concentration [18], the thickness of double electric layer decreases and the nanoparticles aggregates are formed.

To avoid agglomeration at high concentration of nanoparticles it is necessary to decrease the concentration of counterions below critical coagulation concentration via irreversible covalent reaction with, for example, propylene epoxide (PE). However, conducting this process without surfactants, will result in slowly aggregation of the particles,

* Corresponding author. Boreskov Institute of Catalysis Novosibirsk, Lavrentieva 5, 630090, Russia.
E-mail address: stas-yk@catalysis.ru (S.S. Yakushkin).

https://doi.org/10.1016/j.matchemphys.2019.01.003
Received 21 August 2018; Received in revised form 21 December 2018; Accepted 1 January 2019
Available online 04 January 2019
0254-0584/

when instead of solid particles, low-density fractal aggregates, such as gels, will be formed [19]. Therefore, the surfactant is a key factor to obtain high concentration of nanoparticles with narrow size distribution. Moreover, the type and content of surfactant has a great influence not only on the synthesis process but also on the properties of the ferrofluid obtained [10].

Although many ferrofluids are commercially produced using two-stage synthesis [10], the development of simple one-stage techniques for synthesizing magnetite nanoparticles with the desired size and magnetic properties is still a challenge [20]. One of the promising approaches is direct synthesis of a colloid in a media acting as a surfactant and surface-active agent [21,22]. Here, we report a simple one-stage synthesis of Fe_3O_4-based ferrofluids with a controllable particle size distribution using dimethylsulfoxide (DMSO) as a reaction media and surfactant. It allows one to fabricate magnetite-based magnetic liquids, stable to sedimentation in gravity and high magnetic fields, with a narrow particle size distribution in the range of 4–10 nm and a wide range of concentrations in one stage at room temperature without complex precursors and special equipment.

2. Experimental

The reagents used were chemically pure $FeCl_3 \cdot 6H_2O$, $FeCl_2 \cdot 4H_2O$ (Acros Organics, 99 + %), their dehydrated forms, propylene epoxide (PE) C_3H_6O, and DMSO (Panreac, > 99.5%). Ferrofluids were synthesized at room temperature in the inert argon atmosphere. To determine the effect of the synthesis conditions on the particle size distribution, several samples with different (5–80 vol%) water contents in the initial solution were prepared taking into account crystalline hydrates water. Most data were obtained for the samples with water contents of 7.3 vol % (sample FF7) and 25 vol% (sample FF25).

The size distribution, particle morphology and crystal structure were studied by X-ray diffraction (XRD) and transmission electron microscopy (TEM). TEM images were obtained on a JEOL JEM-2010 microscope at an accelerating voltage of 200 kV, which ensured a spatial resolution of 1.4 Å. The nanoparticle size distribution was determined from several microphotographs taken from different sample parts. The XRD analysis was performed on an ARL™ X'TRA powder diffractometer (Thermo Fisher Scientific company) in CuK_α radiation (the wavelength is $\lambda = 1.5418$ Å) with a 2θ scanning step of 0.1° and an accumulation time of 5 s.

Ferromagnetic resonance (FMR) combined with Mössbauer spectroscopy and magnetostatic measurements were used to examine the magnetic and magnetic resonance properties of the ferrofluids. FMR spectra were recorded on a Bruker ELEXSYS 500 radiospectrometer operating in the X-band mode ($\nu = 9.4$ GHz). The samples were placed at the center of a TE_{102} rectangular cavity with a magnetic component of the UHF field perpendicular to the external magnetic field direction. The sample magnetization was measured on a PPMS-6000 vibrating sample magnetometer at temperatures from 4.2 to 300 K. In the measurements, the samples containing 40 wt% of magnetite nanoparticles (FF7) uniformly dispersed in wax were used.

3. Results and discussion

The synthesis procedure begins with dissolving iron chloride hydrates in DMSO or the DMSO-H_2O mixture. To obtain a concentrated sol of isolated nanoparticles, it is necessary to overcome the high concentration of Cl^- anions, which tend to adsorb on the nanoparticle surface with the formation of a double electric layer. The double electric layers of different nanoparticles overlap in the concentrated sol, which leads to agglomeration of nanoparticles. This problem can be solved by irreversible substitution of OH^- anions for Cl^- ones using PE. In turn, OH^- anions are involved in the formation of iron hydroxide complexes. The full reaction scheme is:

$$2\,FeCl_3 + FeCl_2 + 4\,H_2O + 8\,C_3H_6O = Fe_3O_4 + 8\,C_3H_7ClO$$

To ensure the complete replacement of Cl^- ions, PE was added in a 50% excess (PE/Cl = 1.5). After the PE addition the solution color changes from yellow to brown within few minutes. This corresponds to the opening of the epoxide cycle with the formation of iron polyhydroxo complexes (PHC) and chloropropanol. When iron chloride is completely converted to PHCs, the PHC polymerization starts. As is known, DMSO forms sufficiently stable complexes with iron ions [23] and shifts the equilibrium of the system via reducing the degree of PHC polymerization. In the next hour, the solution transforms to a stable gel with the brown color. Further rearrangement of iron PHCs leads to the formation of magnetite nanoparticles, which form a black magnetic fluid within next few hours. If the iron ion concentration in the reaction mixture is higher than 0.38 mol/L, the formation of a gel can be easily observed, while at the lower Fe concentrations, the gel is too unstable and can be destroyed by shaking the reaction mixture.

At this stage of the process, DMSO works as a surfactant, since the interaction between DMSO molecules and the magnetite nanoparticle surface prevents interparticle adhesion and agglomeration. The DMSO adsorption on the surface of nanoparticles stops their growth at a certain size. This results in the formation of ensembles consisting of particles few nanometers in size with a narrow size distribution.

Fig. 1 (inset) shows TEM images of sample FF7 and the particle size distribution. The particles obtained are spherical, well-crystallized, and have an average size of 3.9 nm with a standard deviation of 0.84 nm.

The XRD investigations confirmed the formation of nanoparticles with the magnetite structure (Fig. 1). Color bars in Fig. 1 show the positions of peaks corresponding to the magnetite structure [24]. The small particle size results in broadening of the diffraction peaks. Analysis of the peak width revealed a coherent diffraction region (CDR) size of ~3 nm, which is consistent with the TEM data.

The samples were studied using a Mössbauer spectroscopy technique. Mössbauer spectra of sample FF7 are shown in Fig. 2. In the room-temperature Mössbauer spectrum, a superparamagnetic doublet is detected against the wide background component (Fig. 2), which makes it difficult to unambiguously identify the sample structure. Therefore, we performed additional measurements at 4.2 K.

The data obtained are given in Table 1. The wide relaxation component detected in the spectrum at 300 K along with the doublet can be approximated by a broad single Lorentzian line (Relax), which reflects the particle size distribution. The 4 K Mössbauer spectrum is a sum of two sextets with broad lines, which confirm the role of the particle size distribution. Isomer shifts (IS) of the doublets are slightly different and

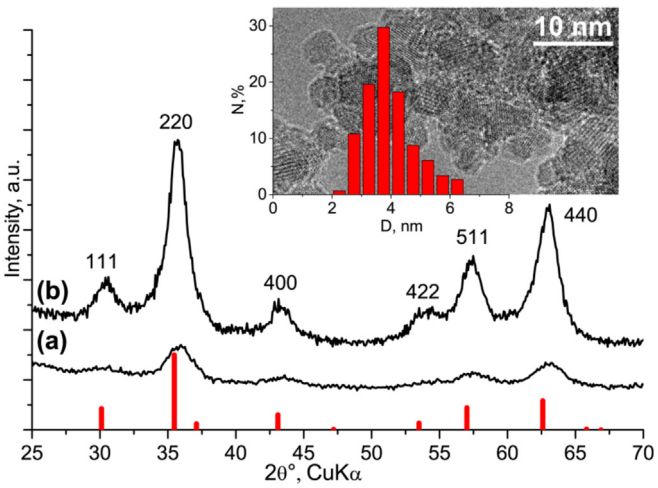

Fig. 1. XRD diffraction patterns of (a) FF7 and (b) FF25 samples. Vertical bars show positions of the magnetite structure peaks (ICSD 26410). Inset: HRTEM image of sample FF7 and particles size distribution.

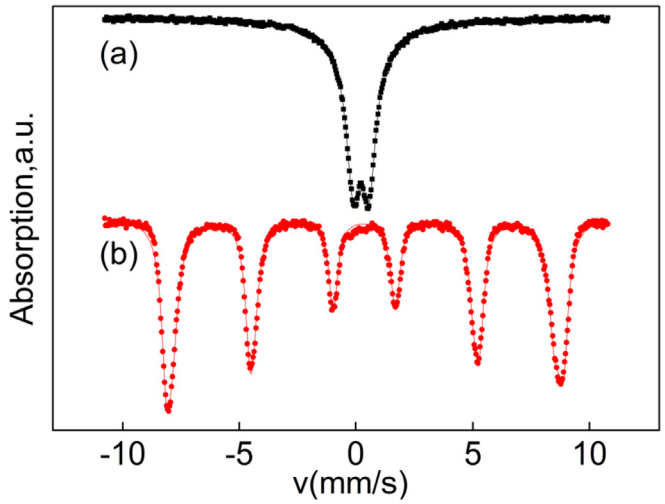

Fig. 2. Mössbauer spectra of sample FF7 at (a) 300 and (b) 4 K.

can be attributed to the variation in the temperature shift in the octahedral and tetrahedral positions. Thus, these sextets can be attributed to the octahedral (S1) and tetrahedral (S2) surrounding.

The iron oxide structure can be determined by analyzing the occupancy of nonequivalent positions. Since magnetite can be presented as $(Fe)[Fe]_2O_4$, the number of octahedral positions in its structure is twice as much as the number of tetrahedral ones [25]. Hence, the ratio between sextet areas corresponding to the octahedral and tetrahedral positions for magnetite nanoparticles should be A_{S1}: A_{S2} = 2: 1. Concerning maghemite, it can be presented as a fully oxidized magnetite with the lattice defects and vacant octahedral sites □ with the formula $(Fe)[Fe_{1.67}□_{0.33}]_2O_4$. Therefore, in maghemite the ratio between sextet areas corresponding to the octahedral and tetrahedral positions should be A_{S1}: A_{S2} = 1.67: 1. This value, however, can change depending on sample preparation conditions. In Ref. [25], a ratio of 1: 1 was reported. According to our data obtained for the samples at 4 K, the ratio between sextet areas is A_{S1}: A_{S2} = 1.94: 1, which confirms the local magnetite structure of nanoparticles.

Fig. 3a shows temperature dependences of magnetization measured in the zero-field cooling (ZFC) and field cooling (FC, in fields of 1000 and 10 Oe) modes for sample FF7 (40 wt% magnetite dispersed in wax). It can be seen that the ZFC M(T) dependences have specific maxima, which can be related to the blocking temperature of particles. In the vicinity of this temperature, the thermomagnetic prehistory manifests itself in a characteristic behavior of the $M(T)_{fc}$ curve, which is indicative of the superparamagnetic state of magnetite nanoparticles. At the same time, a great difference between the blocking temperatures (25 and 115 K at 1000 and 10 Oe, respectively) points out the presence of significant interparticle magnetic couplings, which affect the magnetic properties of the system containing 40 wt% of magnetite nanoparticles [26,27]. This leads to the narrower room-temperature M(H) hysteresis (inset in Fig. 4) with a coercivity of $H_C \approx$ 55 Oe. At lower temperatures, the H_C value increases to about 450 Oe, which is typical of few-nanometer magnetite particles in the blocked state [17,28–31].

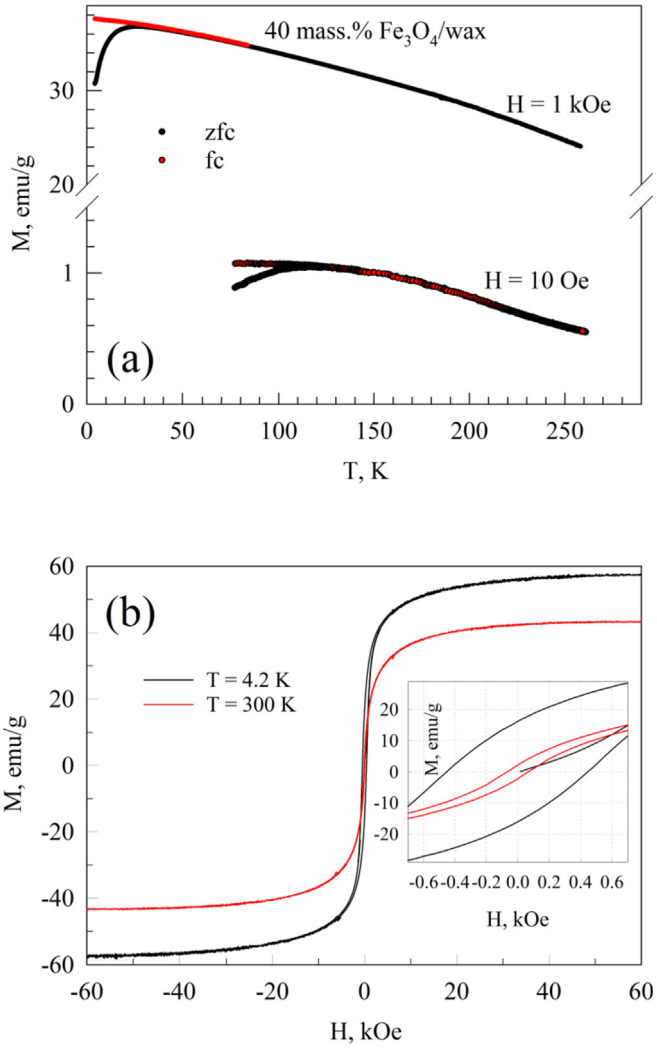

Fig. 3. (a) ZFC and FC temperature dependences of magnetization for sample FF7 (40 wt% in wax). (b) Magnetic hysteresis loops for sample FF7 (40 wt% in wax) at 300 K and 4.4 K. Inset: low-field hysteresis loops.

Using the magnetization curve (Fig. 3b), we can estimate saturation magnetization M_S. At 4.2 K, the saturation magnetization is 58 ± 2 emu/g, which is noticeably lower than the value $M_{S\ bulk} \approx 92$ emu/g for bulk magnetite. This phenomenon is typical of nanosized ferro- and ferromagnetic particles [17,28,29,32]. The decrease in the saturation magnetization is caused by the presence of the so-called magnetic dead layer on the surface of particles that consist of atoms with weak exchange couplings with the core spins and, therefore, are not involved in the formation of the resulting magnetic moment of a particle and often lead to the spin-glass behavior. At room temperature, these surface atoms work as a paramagnetic subsystem [33–35]. Using the magnetization data, we can estimate the magnetic dead layer thickness a from the formula $M_S = M_{S\ bulk}\ (1 - 2a/D)^3$, where D is the nanoparticle size.

Table 1
Parameters of the Mössbauer spectra for sample FF7.

	IS, 0,005 mm/s	H_{hf}, ± 5 kOe	QS, ± 0,02 mm/s	W, ± 0,02 mm/s	Area	position
300 K						
D1	0.338	–	0.66	0.72	0.67	–
Relax	0.367	–	3.60	0.13	0.33	–
4 K						
S1	0.483	530	−0.03	0.44	0.66	[Fe]
S2	0.435	511	−0.00	0.43	0.34	(Fe)

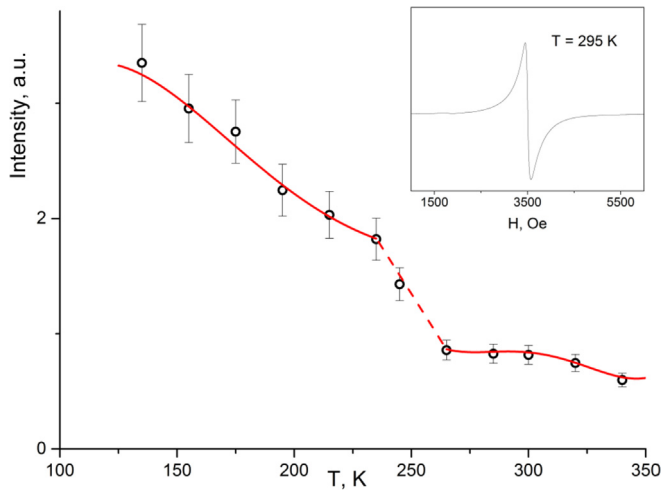

Fig. 4. Temperature dependence of the integral intensity of FMR spectra for sample FF7. Inset: FMR spectrum detected at 295 K.

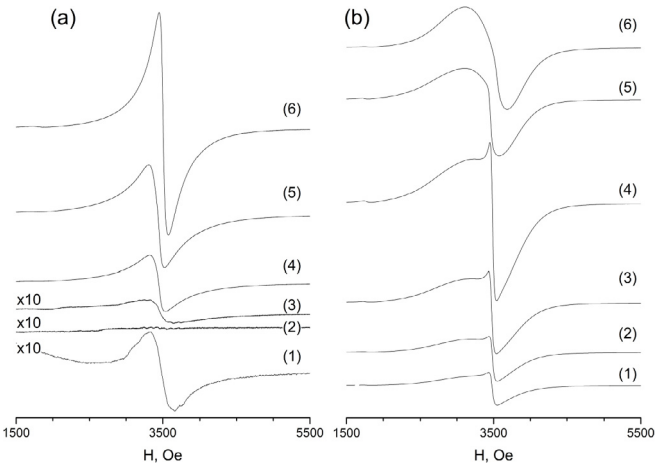

Fig. 5. (a) — FMR spectra detected during the formation of the sample FF7. Initial solution of Fe^{3+} ions – (1); 1 h after the EP addition – (2); 8 h after – (3); 18 h after – (4); 29 h after – (5); 48 h after – (6). The detection temperature is 298 K. (b) — FMR spectra detected during the formation of the sample FF25.18 h after the EP addition – (1); 40 h after – (2); 90 h after – (3); 142 h after – (4); 260 h after – (5); 480 h after – (6) The detection temperature is 298 K.

At an average particle size of $D \approx 4$ nm, we have $a \approx 0.3$ nm. This is significantly lower than a value of 0.7–0.8 nm reported in Refs. [17,29].

The superparamagnetic behavior of nanoparticles agrees well with the FMR data (Fig. 4). The inset in Fig. 4 shows a typical FMR signal for sample FF7 at room temperature, which can be attributed to the superparamagnetic iron oxide nanoparticles. The FMR spectrum shape and intensity depend on the degree of thermal fluctuations of the magnetic moment of each particle in an ensemble at the detection temperature. The temperature dependence of the integral intensity of FMR spectrum (Fig. 4) is consistent with the M(T) behavior (Fig. 3a). At the same time, one can see a feature in the dependence at 220–270 K, which coincides with the DMSO/H_2O solution freezing point. As is known, the behavior of an ensemble of superparamagnetic particles in a liquid solution is significantly different from the case of immobile nanoparticles [36]. This difference is related to the two independent sources of the superparamagnetic nanoparticle fluctuation. When nanoparticles are immobilized in a solid matrix, only the Langevin fluctuations of the magnetic moment direction can occur. Melting of a ferrofluid allows the Brownian motion of nanoparticle and thereby changes the dynamic magnetic properties of a system, which can be detected by the FMR technique.

The initial stages of magnetite nanoparticle formation were studied by the FMR method. The FMR spectra of the samples were detected each 30 min after starting the synthesis. Fig. 5 shows the most characteristic spectra detected during the synthesis. Immediately after adding PE to the Fe(II)/(III) ion-containing solution, the intensity sharply dropped and the resonance absorption related to paramagnetic Fe^{3+} ions completely vanished (Fig. 5a (2)). Near g = 2, we observed a signal consisting of six equidistant nonuniformly broadened lines, which can be attributed to Mn^{2+} ions. As is known, the manganese impurity is frequently met in iron-containing compounds. The Mn^{2+} lines become distinguishable in the FMR spectrum, which is indicative of the disappearance of line broadening under the action of the spin exchange between Mn^{2+} and Fe^{3+} ions. These variations in the spectra point out the formation of antiferromagnetically ordered iron hydroxide-based structures at the initial stage of the particle formation, which is consistent with the available literature data [9].

Then, the nonuniformly broadened resonance signal smoothly grows near g = 2 and is characterized by peak-to-peak width dH_{pp} in the range of 500–1000 Oe. During first 10 h, the signal intensity increases relatively slow, while the signal corresponding to Mn^{2+} ions is still observed. It means that during this period the antiferromagnetic phase (iron PHC) gradually transforms to the ferrimagnetic iron oxide Fe_3O_4. With time, the resonance signal intensity increases by an order of magnitude, while the lines corresponding to paramagnetic Mn^{2+} ions broaden. This behavior corresponds to the occurrence of the significant magnetic field nonuniformity in the local environment of Mn^{2+} ions, which is related to the formation of superparamagnetic nanoparticles in the system. In addition, the spectrum width decreases to ~200 Oe, which suggests a decrease in the structural inhomogeneity. We may conclude that, at this stage, the Fe_3O_4 nanoparticle structure formation is completed.

It is worth noting that, at this stage, during the next 40 + hours, the magnetic nanoparticle size does not increase; otherwise, the spectrum would broaden rather than narrow. The ferrofluid synthesis was almost completed within two days, while the FMR absorption line width continues decreasing down to 85 Oe (Fig. 5a). The interaction of the nanoparticles surface with DMSO molecules apparently plays a decisive role in controlling the size characteristics of the oxide phase. The adsorption of DMSO molecules on the nanoparticle surface inhibits the growth, resulting in the synthesis of a colloid with a narrow particle size distribution. Thus, an important parameter determining the magnetic iron oxide nanoparticle size during the ferrofluid synthesis is the adsorption of DMSO molecules on the surface of nanoparticles formed. Indeed, if the synthesis is performed in a dilute DMSO solution, the samples with the greater average particle size are obtained.

Fig. 5b shows the spectra recorded during the synthesis of a ferrofluid in 25-vol.% H_2O-DMSO solution (sample FF25). The main differences of these spectra from the case of the synthesis in pure DMSO were detected in 10 h after the reaction start. Along with the narrow signal of superparamagnetic particles, the FMR spectra contain a broad component indicating the formation of magnetite nanoparticles about ~7 nm in size.

In the 25% H_2O-DMSO solution, the ferrofluid formation does not stop after two days, in contrast to the case of the low H_2O concentration. In the next 200 h, the narrow absorption line intensity gradually decreases. We may conclude that nanoparticles more than 7 nm in size are formed in the solution during agglomeration. The agglomeration of particles goes slower than their formation, so we obtain a stable colloid only in 20 days after the reaction start. Fig. 6 shows the magnetite nanoparticle average size in the ferrofluid as a function of the water content in the reaction mixture. It can be seen that the increase in the water content in the range of 25–35 vol% leads to a sharp increase in the average particle size. It means that, probably, starting with the 25 vol% water content in the reaction mixture, the layer of DMSO

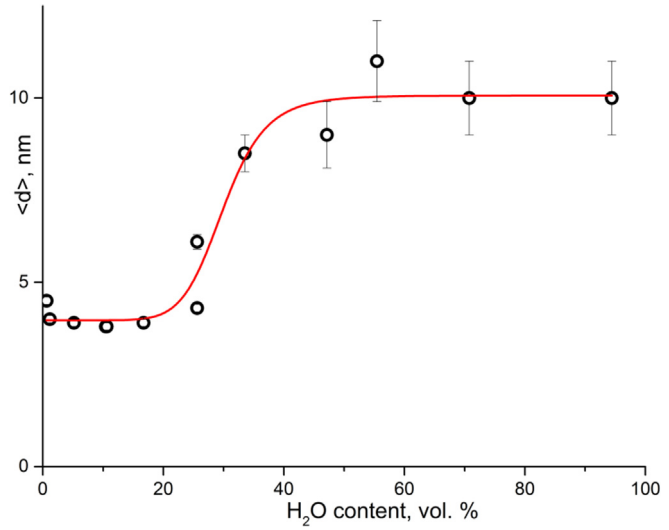

Fig. 6. Average particle size vs H_2O content (vol. %) in the reaction mixture. The solid line is given for clarity.

molecules adsorbed on the nanoparticle surface cannot efficiently inhibit the particle growth. When the water content attains 40 vol%, DMSO weakly affects the particle formation and the average particle size becomes almost the same as in the aqueous solution synthesis [17].

4. Conclusions

The original one-stage method for synthesizing ferrofluids based on magnetite nanoparticles with an average size in the range of 4–10 nm and a narrow size distribution using dimethylsulfoxide as a reaction media was proposed. The advantages of this method, along with the one-stage procedure, are scaling simplicity and availability of the reagents used. This is the first example of synthesizing the stable concentrated magnetite/DMSO sols with a narrow particle size distribution at ambient temperatures without special equipment, expensive precursors, and multicomponent mixtures (surfactant additives).

It was shown that the nanoparticles formed have a magnetite structure and exhibit a superparamagnetic behavior at room temperature. In this case, the increase in the magnetite nanoparticle concentration in a ferrofluid to 40 wt % leads to the room-temperature hysteresis caused by the dipole-dipole interactions of magnetic particles. The nanoparticle saturation magnetization was found to be 66 emu/g at 4.2 K. The magnetic dead layer formed on the nanoparticle surface results in the lower magnetization of magnetite nanoparticle as compared with the bulk phase. The estimation of the magnetic dead layer yielded a thickness of about 0.3 nm. This is significantly smaller than the values obtained previously and indicative of the well-crystallized structure of magnetite nanoparticles.

The FMR study of the ferrofluid formation showed that the DMSO adsorption on the nanoparticle surface prevents the particle agglomeration and growth. The dilution of DMSO with water leads to a significant increase in the iron oxide nanoparticle size. Thus, the competitive adsorption of DMSO molecules on the nanoparticle surface during the synthesis is an effective tool for precise tuning of the size characteristics of the magnetic phase.

Compliance with Ethical Standards

Conflicts of interest

The authors declare that they have no conflict of interest.

Acknowledgements

This work was supported by the Russian Science Foundation, project no. 17-12-01111.

References

[1] J.D.A. Gomes, M.H. Sousa, F.A. Tourinho, R. Aquino, G.J. Da Silva, J. Depeyrot, E. Dubois, R. Perzynski, Synthesis of core-shell ferrite nanoparticles for ferrofluids: chemical and magnetic analysis, J. Phys. Chem. C 112 (2008) 6220–6227, https://doi.org/10.1021/jp7097608.
[2] D. Zins, V. Cabuil, R. Massart, Synthesis of Core − Shell ferrite nanoparticles for ferrofluids: chemical and magnetic analysis, J. Mol. Liq. 83 (2008) 217–232, https://doi.org/10.1021/jp7097608.
[3] W. Cai, J. Wan, Facile synthesis of superparamagnetic magnetite nanoparticles in liquid polyols, J. Colloid Interface Sci. 305 (2007) 366–370, https://doi.org/10.1016/j.jcis.2006.10.023.
[4] D. Milivojević, B. Babić-Stojić, V. Jokanović, Z. Jagličić, D. Makovec, N. Jović, Magnetic properties of ultrasmall iron-oxide nanoparticles, J. Alloy. Comp. 595 (2014) 153–157, https://doi.org/10.1016/j.jallcom.2014.01.112.
[5] G. Goloverda, B. Jackson, C. Kidd, V. Kolesnichenko, Synthesis of ultrasmall magnetic iron oxide nanoparticles and study of their colloid and surface chemistry, J. Magn. Magn Mater. 321 (2009) 1372–1376, https://doi.org/10.1016/j.jmmm.2009.02.041.
[6] H. Hu, H. Yang, P. Huang, D. Cui, Y. Peng, J. Zhang, F. Lu, J. Lian, D. Shi, Unique role of ionic liquid in microwave-assisted synthesis of monodisperse magnetite nanoparticles, Chem. Commun. 46 (2010) 3866, https://doi.org/10.1039/b927321b.
[7] A.E. Berkowitz, J.A. Lahut, I.S. Jacobs, L.M. Levinson, D.W. Forester, Spin pinning at ferrite-organic interfaces, Phys. Rev. Lett. 34 (1975) 594–597, https://doi.org/10.1103/PhysRevLett.34.594.
[8] S.J. Doktycz, K.S. Suslick, Interparticle collisions driven by ultrasound, Science 247 (1990) 1067–1069, https://doi.org/10.1126/science.2309118.
[9] A.S. Drozdov, V. Ivanovski, D. Avnir, V.V. Vinogradov, A universal magnetic ferrofluid: nanomagnetite stable hydrosol with no added dispersants and at neutral pH, J. Colloid Interface Sci. 468 (2016) 307–312, https://doi.org/10.1016/j.jcis.2016.01.061.
[10] A. Joseph, S. Mathew, Ferrofluids: synthetic strategies, stabilization, physicochemical features, characterization, and applications, ChemPlusChem 79 (2014) 1382–1420, https://doi.org/10.1002/cplu.201402202.
[11] M.T. López-López, J.D.G. Durán, A.V. Delgado, F. González-Caballero, Stability and magnetic characterization of oleate-covered magnetite ferrofluids in different nonpolar carriers, J. Colloid Interface Sci. 291 (2005) 144–151, https://doi.org/10.1016/j.jcis.2005.04.099.
[12] D. Maity, D.C. Agrawal, Synthesis of iron oxide nanoparticles under oxidizing environment and their stabilization in aqueous and non-aqueous media, J. Magn. Magn Mater. 308 (2007) 46–55, https://doi.org/10.1016/j.jmmm.2006.05.001.
[13] A.S. Teja, P.-Y. Koh, Synthesis, properties, and applications of magnetic iron oxide nanoparticles, Prog. Cryst. Growth Char. Mater. 55 (2009) 22–45, https://doi.org/10.1016/j.pcrysgrow.2008.08.003.
[14] A. Nikitin, M. Fedorova, V. Naumenko, I. Shchetinin, M. Abakumov, A. Erofeev, P. Gorelkin, G. Meshkov, E. Beloglazkina, Y. Ivanenkov, N. Klyachko, Y. Golovin, A. Savchenko, A. Majouga, Synthesis, characterization and MRI application of magnetite water-soluble cubic nanoparticles, J. Magn. Magn Mater. 441 (2017) 6–13, https://doi.org/10.1016/j.jmmm.2017.05.039.
[15] J.-H. Wu, S.P. Ko, H.-L. Liu, S. Kim, J.-S. Ju, Y.K. Kim, Sub 5 nm magnetite nanoparticles: synthesis, microstructure, and magnetic properties, Mater. Lett. 61 (2007) 3124–3129, https://doi.org/10.1016/j.matlet.2006.11.032.
[16] S.V. Gopal, R. Mini, V.B. Jothy, I.H. Joe, Synthesis and characterization of iron oxide nanoparticles using DMSO as a stabilizer, Mater. Today Proc, Elsevier Ltd., 2015, pp. 1051–1055, , https://doi.org/10.1016/j.matpr.2015.06.036.
[17] V.L. Kirillov, D.A. Balaev, S.V. Semenov, K.A. Shaikhutdinov, O.N. Martyanov, Size control in the formation of magnetite nanoparticles in the presence of citrate ions, Mater. Chem. Phys. 145 (2014) 75–81, https://doi.org/10.1016/j.matchemphys.2014.01.036.
[18] T. Tadros (Ed.), Colloid Stability: the Role of Surface Forces - Part I, Viley-VCH Verlag GmbH, Weinheim, 2007.
[19] H. Cui, Y. Jia, W. Ren, W. Wang, Facile and ultra large scale synthesis of nearly monodispersed CoFe2O4 nanoparticles by a low temperature sol–gel route, J. Sol. Gel Sci. Technol. 55 (2010) 36–40, https://doi.org/10.1007/s10971-010-2210-0.
[20] W. Yu, H. Xie, A review on nanofluids: preparation, stability mechanisms, and applications, J. Nanomater. 2012 (2012) 1–17, https://doi.org/10.1155/2012/435873.
[21] Z. Li, Q. Sun, M. Gao, Preparation of water-soluble magnetite nanocrystals from hydrated ferric salts in 2-pyrrolidone: mechanism leading to Fe3O4, Angew. Chem. Int. Ed. 44 (2004) 123–126, https://doi.org/10.1002/anie.200460715.
[22] C.Y. Wang, J.M. Hong, G. Chen, Y. Zhang, N. Gu, Facile method to synthesize oleic acid-capped magnetite nanoparticles, Chin. Chem. Lett. 21 (2010) 179–182, https://doi.org/10.1016/j.cclet.2009.10.024.
[23] M.V. Twigg, J. Burgess, Iron, Compr. Coord. Chem. II, Elsevier, 2003, pp. 403–553, , https://doi.org/10.1016/B0-08-043748-6/04208-0.
[24] M.E. Fleet, The structure of magnetite, Acta Crystallogr. Sect. B Struct. Crystallogr. Cryst. Chem. 37 (1981) 917–920, https://doi.org/10.1107/S0567740881004597.
[25] K. Woo, J. Hong, S. Choi, H.-W. Lee, J.-P. Ahn, C.S. Kim, S.W. Lee, Easy synthesis

and magnetic properties of iron oxide nanoparticles, Chem. Mater. 16 (2004) 2814–2818, https://doi.org/10.1021/cm049552x.
[26] W.C. Nunes, L.M. Socolovsky, J.C. Denardin, F. Cebollada, A.L. Brandl, M. Knobel, Role of magnetic interparticle coupling on the field dependence of the superparamagnetic relaxation time, Phys. Rev. B 72 (2005) 212413, , https://doi.org/10.1103/PhysRevB.72.212413.
[27] M. Knobel, W.C. Nunes, H. Winnischofer, T.C.R. Rocha, L.M. Socolovsky, C.L. Mayorga, D. Zanchet, Effects of magnetic interparticle coupling on the blocking temperature of ferromagnetic nanoparticle arrays, J. Non-Cryst. Solids 353 (2007) 743–747, https://doi.org/10.1016/j.jnoncrysol.2006.12.037.
[28] G.F. Goya, T.S. Berquó, F.C. Fonseca, M.P. Morales, Static and dynamic magnetic properties of spherical magnetite nanoparticles, J. Appl. Phys. 94 (2003) 3520–3528, https://doi.org/10.1063/1.1599959.
[29] P. Dutta, S. Pal, M.S. Seehra, N. Shah, G.P. Huffman, Size dependence of magnetic parameters and surface disorder in magnetite nanoparticles, J. Appl. Phys. 105 (2009) 10–13, https://doi.org/10.1063/1.3055272.
[30] S. Ayyappan, G. Panneerselvam, M.P. Antony, N.V. Rama Rao, N. Thirumurugan, A. Bharathi, J. Philip, Effect of initial particle size on phase transformation temperature of surfactant capped Fe $_3$ O $_4$ nanoparticles, J. Appl. Phys. 109 (2011) 084303, , https://doi.org/10.1063/1.3564964.
[31] D.A. Balaev, S.V. Semenov, A.A. Dubrovskiy, S.S. Yakushkin, V.L. Kirillov, O.N. Martyanov, Superparamagnetic blocking of an ensemble of magnetite nanoparticles upon interparticle interactions, J. Magn. Magn Mater. 440 (2017) 199–202, https://doi.org/10.1016/j.jmmm.2016.12.046.
[32] A. Millan, A. Urtizberea, N.J.O. Silva, F. Palacio, V.S. Amaral, E. Snoeck, V. Serin, Surface effects in maghemite nanoparticles, J. Magn. Magn Mater. 312 (2007), https://doi.org/10.1016/j.jmmm.2006.09.011.
[33] H. Wang, T. Zhu, K. Zhao, W.N. Wang, C.S. Wang, Y.J. Wang, W.S. Zhan, Surface spin glass and exchange bias in Fe3O4 nanoparticles compacted under high pressure, Phys. Rev. B 70 (2004) 092409, , https://doi.org/10.1103/PhysRevB.70.092409.
[34] A.A. Dubrovskiy, D.A. Balaev, K.A. Shaykhutdinov, O.A. Bayukov, O.N. Pletnev, S.S. Yakushkin, G.A. Bukhtiyarova, O.N. Martyanov, Size effects in the magnetic properties of ε-Fe2O3 nanoparticles, J. Appl. Phys. 118 (2015) 213901, , https://doi.org/10.1063/1.4936838.
[35] D.A. Balaev, I.S. Poperechny, A.A. Krasikov, K.A. Shaikhutdinov, A.A. Dubrovskiy, S.I. Popkov, A.D. Balaev, S.S. Yakushkin, G.A. Bukhtiyarova, O.N. Martyanov, Y.L. Raikher, Dynamic magnetization of ε -Fe2O3 in pulse field: evidence of surface effect, J. Appl. Phys. 117 (2015), https://doi.org/10.1063/1.4907586.
[36] Y.L. Raikher, V.I. Stepanov, Ferromagnetic resonance in a suspension of single-domain particles, Phys. Rev. B 50 (1994) 6250–6259, https://doi.org/10.1103/PhysRevB.50.6250.